# Structure of Cationic Starch (CS)/Anionic Surfactant Complexes Studied by Small-Angle X-ray Scattering (SAXS)

**Juha Merta,*,† Mika Torkkeli,‡ Teemu Ikonen,‡ Ritva Serimaa,‡ and Per Stenius†**

*Laboratory of Forest Products Chemistry, Department of Forest Products Technology,*
*Helsinki University of Technology, P.O. Box 6300, FIN-02015 HUT, Espoo, Finland; and*
*Laboratory of X-ray Physics, Department of Physics, University of Helsinki, Helsinki, Finland*

*Received October 17, 2000; Revised Manuscript Received January 30, 2001*

ABSTRACT: The structure of lyotropic liquid crystalline or gellike phases formed in cationic starch (CS)/ anionic surfactant/water systems in the temperature range 25−80 °C has been investigated by small-angle X-ray scattering. The surfactants were sodium dodecyl sulfate (SDS), sodium decanoate (NaDe), sodium dodecanoate (NaDod), sodium palmitate (NaPal), sodium oleate (NaOl), and sodium erucate (NaEr). The phases were in equilibrium with aqueous solutions at 60 °C and contained 15−25 wt % of CS and 10−30 wt % of surfactant, depending on the charge density of the CS and the chain length of the surfactant. The phases consist of CS/surfactant aggregates arranged in long-range structures similar to lyotropic mesophases formed by the pure surfactants alone, but they separate from aqueous solutions at much lower surfactant concentrations. When the charge density of the CS is low or the surfactant hydrocarbon chain is short, cubic or hexagonal phases are formed. As expected, the formation of lamellar phase is promoted by increasing these parameters. Temperature affects the stability of the phases and their structure. At high temperatures the long-range order breaks down, and the phases are akin to concentrated micellar CS/surfactant solutions.

## Introduction

The present understanding of polymer/surfactant interactions in aqueous solution has been summarized in several reviews, for example.[1−4] Many investigations have focused on aggregate structure in dilute solution, i.e., systems in which phase separation does not occur. The general picture emerging from these studies is that in dilute solution the surfactant molecules adsorb to polymer chains as micellar or micelle-like clusters. A general phenomenon in systems of polyelectrolyte and oppositely charged surfactant is that complexes of these components separate as a water-swollen phase in equilibrium with very dilute aqueous solution.

Generally, the rich phase behavior of surfactants in water is also characteristic of polyelectrolyte−surfactant complexes in contact with water. In an early paper, Harada and Nozakura[5] describe the formation of layered structures in polyvinyl sulfate (PVS)/cetyltrimethylammonium bromide and 1−4-ionene/sodium dodecyl sulfate (SDS) systems. More extensive studies of *x,y*-ionene/ SDS and PVS/*n*-alkylpyridinium surfactants systems have recently been reported in a series of papers.[6,7] Kabanov and co-workers[8−12] observed that complexes of sodium poly(acrylate) gel and alkyltrimethylammonium bromides form lamellar structures. Hansson[13] found that a cubic phase was formed by sodium poly-(acrylate) and dodecyltrimethylammonium bromide. Ilekti et al.[14] studied sodium poly(acrylate)/cetyltrimethylammonium bromide complexes and found that they form hexagonal structures and that the ionic compositions of the concentrated and dilute phase have significant effect on the phase behavior. Kosmella et al.[15] and Ruppelt et al.[16] found that the intercalation of sodium poly(acrylate) into mesophases formed by alkyltrimethylammonium bromides induced some disordering, but

did not substantially affect the phase structures. Very recently Zhou et al.[17] observed long-range order in complexes of poly(sodium methacrylate-*co*-*N*-isopropylacrylamide) and poly(styrenesulfonate) with tetradecyl-, hexadecyl-, or dodecyltrimethylammonium bromide.[18]

A characteristic of the complexes discussed in this paper is that they contain a very hydrophilic carbohydrate polymer associated with oppositely charged surfactants. Thus, we expect the predominant driving forces for the self-assembly of surfactant molecules in these complexes to be hydrophobic interactions between the hydrocarbon chains of the surfactant and electrostatic interactions between charged segments of the polymer and the headgroups of the surfactant.

This paper is part of a systematic study of systems of cationic starch and anionic surfactants. Previously, we have reported on interactions,[19] aggregate formation,[20] and rheological properties of the complex phase in these systems.[21] Our goal is to evaluate the structure of the phases in equilibrium with very dilute aqueous solution. Goddard et al. investigated the interactions between surfactants with cationized cellulose and the rheology of the complexes[22,23] but to our knowledge our studies are the first investigations reported of cationic starch/ anionic surfactant systems.

## Experimental Section

**Materials. Cationic starch** (CS) (2-hydroxy-3-trimethylammoniumpropyl starch) with different degrees of substitution (DS) (0.42, 0.72, 0.80) was synthesized from potato starch by Raisio Chemicals, Raisio, Finland. The DS was calculated from the nitrogen content.

Before cationization, the starch was partially depolymerized by reaction with sodium hypochlorite in a slurry of the starch at controlled pH and temperature.[24] The acidic reaction product was neutralized with dilute NaOH. When the oxidation had reached the required level, the reaction was stopped by lowering the pH, and excess hypochlorite was decomposed by addition of sodium bisulfite.

---

† Helsinki University of Technology.
‡ University of Helsinki.

**Table 1. Properties of Cationic Starch Samples**

| degree of substitution[c] | mol wt range ($M_w$)[a] | particle size range ($\mu$m)[b] |
|---|---|---|
| 0.42 | $(0.5-9) \times 10^4$ | 0.01-0.5 |
| 0.72 | $(0.4-9) \times 10^4$ | 0.01-0.6 |
| 0.80 | $(0.5-9) \times 10^4$ | 0.01-0.7 |

[a] By GPC. [b] By light scattering. [c] As reported by the manufacturer.

Low molecular weight components and salt were removed by filtration of the cationized starch in a Filtron Technology Corp., Minisette, tangential flow ultrafiltration system, using a membrane with cutoff 8000. The starch was dissolved in water by heating the starch/water mixture in an autoclave for 30 min at 120 °C. All solutions were prepared at least 24 h before measurements. Some properties of the CS samples are summarized in Table 1.

**Surfactants.** The alkanoates (sodium octanoate, $C_7H_{15}$-COONa (NaOct), sodium decanoate, $C_9H_{19}$COONa (NaDe), sodium dodecanoate, $C_{11}H_{23}$COONa, (NaDod), sodium palmitate (sodium hexadecanoate), $C_{15}H_{31}$COONa, (NaPal), sodium oleate, (sodium *cis*-9-octadecenoate), $C_9H_{18}$=$C_8H_{15}$COONa, (NaOl) and sodium erucate (sodium *cis*-13-docosenoate), $C_9H_{18}$=$C_{12}H_{23}$COONa, (NaEr) were synthesized by neutralizing the corresponding acid (of purum quality from Fluka Ag or Sigma) in alcoholic solution with sodium hydroxide. The salts were purified by recrystallization from acetone. Sodium dodecyl sulfate (SDS), analytical grade, was from Fluka Ag and was further purified by recrystallization from ethanol. It showed no minimum in surface tension below the critical micelle concentration.

**Other Chemicals.** The water was ion exchanged and distilled. All other chemicals were analytical grade and were used without further purification.

**Methods. X-ray Scattering.** Small angle X−ray scattering (SAXS) measurements were performed using Cu Kα ($\lambda = 1.542$ Å) radiation monochromatized with a Ni filter and a totally reflecting glass block (Huber small-angle chamber 701). The intensity curves were measured using a linear position sensitive detector (Mbraun OED-50 M).

The fine focus ($0.4 \times 10$ mm) X-ray tube is placed in a point-focus position. The beam is reduced in the vertical direction with a 1 mm slit in front of the sample and a triangular slit in front of the detector. The scattering vector lies in the horizontal direction and its length is defined as

$$k = \frac{4\pi}{\lambda}\sin\theta \quad (1)$$

where $\lambda$ is the wavelength and $2\theta$ is the scattering angle. The $k$ range was from 0.03 to 0.65 Å$^{-1}$. The full width at half-maximum height of the instrumental broadening function was 0.01 Å$^{-1}$ in the horizontal direction and 0.08 Å$^{-1}$ in the vertical direction. Thus, the geometry is considered as pointlike, and apart from the detector height and response profile, no further corrections were applied. The background scattering was measured separately and subtracted from the intensity curves.

**Sample Preparation.** Weighed amounts of cationic starch, surfactants, and distilled water were added to tightly closed test tubes. The tubes were equilibrated by continuously turning them over in a thermostat at 333 K (for CS/SDS the temperature was 298 K) for 7 days. This resulted in the formation as a complex phase dispersed in aqueous solution. The charge neutrality of the complexes was verified by measuring the electrophoretic mobility of the dispersed particles.

The solution and complex phases were separated by centrifugation for 30 min at 1600*g*. After centrifugation, the samples were again allowed to equilibrate at the same temperature for 7 days. Then the phases were separated by careful decantation of the solution. The dry content of the complex phase was determined by weighing. The CS content was determined by Kjeldahl analysis of the amount of nitrogen.[25] The amount of surfactant was calculated as the difference between the amount of starch and the total amount of dry matter in the samples.

The composition of the supernatant phase was analyzed by determining the CS concentration by ordinary spectrophotometric methods used commonly to determine the total carbohydrate content. The amount of surfactant in the supernatant phase was determined by a standard gas chromatographic method of carboxylic acid analysis. As a result of neutralization of the cationic starch with surfactant, the two phases in equilibrium will also contain some NaCl. The NaCl concentration of separate phases was not determined, but total salt content is, of course, directly dependent on the amount of associated surfactant.

For the SAXS measurements, a small amount (ca. 20 mg) of the complex phase was sealed in a steel ring between 13 $\mu$m poly(imide) windows to prevent dehumidification and pressed against a hot plate (LINKAM TP93 hot stage) which has a small aperture for an X-ray beam. Thus, all samples were first equilibrated with aqueous solutions at 333 K (or 298K for CS/SDS) and then thermostated at different temperatures during the SAXS measurements.

**Interpretation of SAXS.** The SAXS method, used to resolve periodic structures in these complexes, is essentially X-ray powder diffraction. In this technique the sample is assumed to contain small crystallites at random orientations. Thus, when monochromatized X-rays are collimated on the sample, we should observe sharp maxima in the scattered intensity whenever the length of the scattering vector $k$ matches any of the reciprocal lattice vectors. If a sufficient number of these peaks is observed, their relative positions on the $k$-axis unambiguously reveal the periodicity of the structure. The actual arrangements of aggregates within the unit cells is, in turn, reflected in the relative peak intensities.

The condition of a sufficient number of reflections is not met with these mesoscopic phases. Thus, the results should be taken as suggestive and ruling out certain alternatives. Fortunately, the structures that are encountered seem to fall to the following simple categories: the lamellar (flat micelles), the two-dimensional hexagonal (cylindrical micelles) or the cubic phase (closed micelles or flat continuous micelles).

The lamellar phase is characterized by an equidistant sequence of reflections $k_n = 2\pi n/L$, where $L$ is the lamellar period and $n = 1,2,3, \ldots$. In both the 2-D and 3-D cases the reflection positions follow a $\sqrt{(n)}$ sequence. In the 2-D hexagonal case the first values are $n = 1, 3, 4, 7, 9, 12, 13, \ldots$, whereas cubic reflections occur at positions $n = h^2 + k^2 + l^2$ where $h$, $k$, and $l$ are whole numbers. There are 36 different space groups of cubic symmetry, with distinct conditions for allowed ($hkl$) combinations.[26] The cubic space groups come in three families: simple cubic (SC), body-centered cubic (bcc) and face-centered cubic (fcc).

**Electrophoretic mobilities** ($\zeta$ potentials) were measured with a Coulter Electronics DELSA 440, Doppler electrophoretic light scattering analyzer. All measurements were performed at constant ionic strength.

## Results

**The Effect of Surfactant Chain Length.** The results of SAXS measurements of all CS/surfactant complexes are collected in Table 2, including the positions of the diffraction peaks and the phase structures inferred from the diffraction pattern.

**CS/NaEr.** The solid curve in Figure 1 shows the intensity of SAXS from the complex phase prepared by mixing CS and NaEr so that neutral particles are formed. The two reflections occurring at $k = 0.117$ and 0.234 Å$^{-1}$ (see Table 2) suggest a lamellar structure. Comparison can be made with the phase formed by pure surfactant with 15−25 wt % of water at room temperature. The two structures are very similar, and the long period (54 Å) is very close to the thickness of an erucate bilayer.

**Table 2. Effect of Temperature on the Structure of CS/Surfactant Complexes**[a]

| surfactant | peak positions (1/Å) | structure of complex | lattice constant (Å) |
|---|---|---|---|
| **SDS** | | | |
| rt | 0.154, 0.274 | 2-D hexagonal | 46.0 |
| +40 °C | 0.155, 0.273 | 2-D hexagonal | 46.0 |
| +60 °C | 0.159, 0.278 | 2-D hexagonal | 45.2 |
| +80 °C | 0.167, 0.296, 0.338 | 2-D hexagonal | 42.9 |
| **NaDe** | | | |
| rt | 0.173 | micellar | 36.0 |
| +40 °C | 0.175 | micellar | 36.0 |
| +60 °C | 0.176 | micellar | 36.0 |
| +80 °C | 0.180, 0.195 | micellar | 33.0 |
| **NaDod** | | | |
| rt | 0.137, 0.145, 0.155, 0.199, 0.235, 0,255 | HCP | $a = 53.0$, $c = 87.0$ |
| +40 °C | 0.140, 0.145, 0.160, 0.208, 0.251, 0.310 | HCP | $a = 50.0$, $c = 82.0$ |
| +60 °C | 0.144, 0.162, 0.177, 0.296 | intermediate between HCP and cubic (pm3n) | |
| +80 °C | 0.144, 0.162, 0.177, 0.296 | cubic (pm3n) | 87.0 |
| **NaPal** | | | |
| rt | 0.106, 0.118, 0.130, 0.151, 0.219, 0.244, 0.305, 0.461 | separate lamellar and cubic (pm3n) | 41.0 (lam.), 118 (cub.) |
| +40 °C | 0.132, 0.228, 0.264 | 2-D hexagonal | 55.0 |
| +60 °C | 0.135, 0.230, 0.273 | 2-D hexagonal | 53.1 |
| +80 °C | 0.138, 0.237, 0.276 | 2-D hexagonal | 52.6 |
| **NaOl** | | | |
| rt | 0.134, 0.228, 0.271 | 2-D hexagonal | 54.0 |
| +40 °C | 0.130, 0.230, 0.268 | 2-D hexagonal | 54.1 |
| +60 °C | 0.138, 0.230, 0.273 | 2-D hexagonal | 53.1 |
| +80 °C | 0.139, 0.250, 0.284 | 2-D hexagonal | 51.1 |
| **NaEr** | | | |
| rt | 0.117, 0.234 | lamellar | 54.0 |
| +40 °C | 0.113, 0.234 | lamellar | 53.7 |
| +60 °C | 0.116, 0.237 | lamellar | 53.0 |
| +80 °C | 0.120, 0.141, 0.243, 0.292 | two lamellar phases | 51.7 and 43.0 |

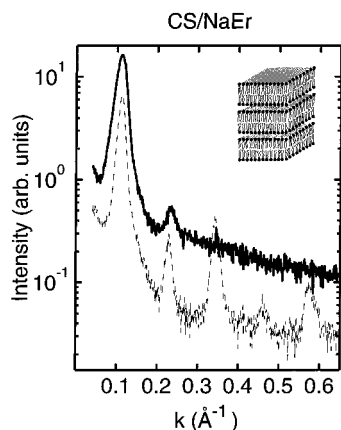[a] The degree of substitution of CS is 0.80. rt = room temperature.



**Figure 1.** SAXS intensity of the neutral CS/NaEr/water system at 25 °C. The dashed curve shows the intensity of the NaEr mixed with 19 wt % water. The DS of starch was 0.80. The water content of gel was 49 wt % at 60 °C. The inset shows a schematic picture of the phase structure.



**Figure 2.** SAXS intensity of the neutral CS/Ol complex at 25 °C. The vertical lines show expected reflections for $R = 18$ Å cylinders in a 2-dimensional hexagonal lattice with a lattice constant 54.4 Å. The model intensity is not in relative scale with the measured data. The dashed curve shows the contribution of the particle scattering factor to the main diffraction lines. The DS of starch was 0.80. The water content of gel was 55 wt % at 60 °C. The inset shows a schematic picture of the phase structure.

**CS/NaOl.** Figure 2 shows the corresponding SAXS intensity curve of a shorter–chain surfactant, NaOl. Distinct reflections occur at $k = 0.134$ and $0.271$ Å$^{-1}$. Between these, a third, not very distinct reflection occurs at $\approx \sqrt{3} \times$ the angle of the first reflection. A likely structure of this system is a two-dimensional hexagonal array of cylindrical micelles. In the 2-D hexagonal phase the first (10) reflection is at position $k = 4\pi/a\sqrt{3}$ where $a$ is the unit cell parameter, which is also equal to the distance between the cylindrical micelles. This gives $a = 54.0$ Å. There are also indications of broad maxima and minima at $k = 0.3$ and $0.4$ Å$^{-1}$ which, if interpreted as scattering from cylindrical particles, suggest a radius of about 18 Å. With this assumption, peak intensities as represented by the tips of the thin vertical lines in Figure 2 are expected. The dashed curve shows the
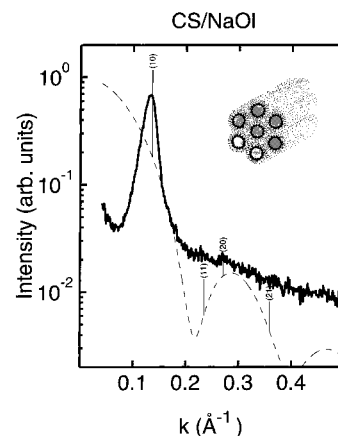
contribution of the particle scattering factor to these diffraction lines. The weak (11) reflection is in line with the proposed model.

**CS/NaPal.** Figure 3 shows the intensity curve for the CS/Pal complex at room temperature. Several distinct reflections occur. As with erucate, comparison with the phase formed in pure NaPal in 15−25 wt % of water is in order. Three positions and relative intensities match with the NaPal/water hydrate, which has a layered crystalline structure. The remaining three reflections at smaller angle (between $k = 0.10$ and $0.13$ Å$^{-1}$) suggest a more complex structure of the system. Their
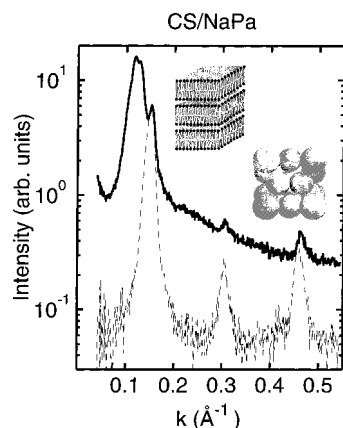
**Figure 3.** SAXS intensity of the neutral CS/Pal complex at 25 °C. The dashed curve shows the intensity of the NaPal mixed with 21 wt % water. The DS of starch was 0.80. The water content of gel was 54 wt % at 60 °C. The inset shows a schematic picture of the phase structures.
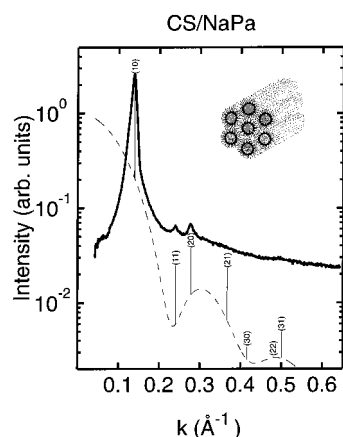


**Figure 4.** SAXS intensity of the neutral CS/Pal complex at 55 °C. The vertical lines show expected reflections similarly to Figure 2. The DS of starch was 0.80. The water content of gel was 54 wt % at 60 °C. The inset shows a schematic picture of the phase structure.

relative positions are close to $\sqrt{4}:\sqrt{5}:\sqrt{6}$. Samples giving this type of intensity curves are frequently assigned space group 223 (*pm3n*) and three reflections are then indexed as (200), (210) and (211). Two structural models have been proposed. Both place spherical micelles at the corner and center positions (0, 0, 0) and ($^1/_2$, $^1/_2$, $^1/_2$) in the unit cell. They differ in the form of the six micelles at positions (0, $^1/_2$, $^1/_4$), (0, $^1/_2$, $^3/_4$), (+ cyclic permutations). In the first case[27] the micelles are rod-shaped but closed; in the second case,[28] they are cross-shaped and extended to form a continuous 3-D network. Fontell et al.[29] found that the structure of the cubic phase of pure NaPal is the same as in solid oxygen and nitrogen, thus here with short rodlike micelles. So there should be only "closed" micelles. In any case, the closest distance between the micelles is $a/2$ and the lattice period is $a = 116$. Although the complexes were prepared at temperatures substantially higher than the Krafft temperature (313 K[30]) of NaPal, the occurrence of this mixture is not surprising, considering the rather high melting point of the NaPal, which, thus, may be partially present as a crystalline hydrate.

To verify this effect of crystallization, further measurements were performed at temperatures above 40–50 °C. Figure 4 gives the scattering intensity at 55 °C. On heating, both the hydrate peaks and the first two of
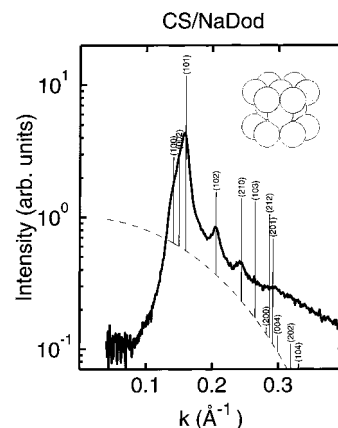


**Figure 5.** CS/Dod complex at 25 °C. The vertical lines represent expected reflection heights and positions for a hcp lattice with lattice constant 51.4 Å and $R = 10.5$ Å spheres at every lattice point. The DS of starch was 0.80. The water content of gel was 64 wt % at 60 °C. The inset shows a schematic picture of the phase structure.

the reflections at smaller angle gradually decrease, while the remaining reflection develops into the (10) reflection of two-dimensional hexagonal ordering, very much like in the case of CS/Ol. The observed epitaxial relationship (211) − (10) has been documented to occur in phase transition between the 2-D hexagonal and the bicontinuous cubic *Ia3d* phase.[31] The lattice parameter (55 Å) and cylinder size (17 Å) is slightly smaller than that for NaOl. The transition from the system containing crystalline hydrate is completely reversible.

**CS/NaDod.** Figure 5 shows the scattering intensity from the CS/Dod complex phase at room temperature. The fact that NaDod has a shorter chain than the previously described surfactants is reflected in the scattering curve which has three well-defined main peaks. The best match is obtained by assuming a hexagonally close-packed (hcp) lattice. The hcp lattice alongside with the fcc represents the two closest packing modes of spheres in three dimensions. The unit cell of hcp is not cubic but hexagonal, and may be constructed from the 2-D hexagonal unit cell with addition of a third perpendicular axis *c*. For the ideal unit cell the ratio is $c/a = \sqrt{(^8/_3)} \sim 1.633$. Under this condition, the reflections occur at $(2\pi/a\sqrt{24})\sqrt{n}$ with $n = 32, 36, 41, 68, 96, 113, \ldots$. The observed reflections follow quite closely these ideal positions, and the experimental ratio is $c/a \sim 1.615$. It seems then fair to assume that the structure consists of spherical micelles stacked in 2-D close packed layers. In every second layer, the micelles are directly on top of each other, while neighboring layers are displaced to the center positions of the triangular net formed by the 2-D hexagonal layer. Thus, each micelle has 12 neighbors approximately at distance $a = 51.4$ Å. There is also indication of a minimum in the scattering curve at $k = 0.43^{-1}$ (outside the range of Figure 5), which would suggest the radius to be 11 Å. Figure 5 also shows the theoretically expected reflections corresponding to the particle dimension for this model, corresponding to the observed particle dimensions (drawn with the dashed line). Of the most notable reflections, (103) and (212) do not appear as strong as expected. This may be due to either strong displacement disorder between the close-packed layers along the *c* axis[32] or due to stronger thermal motion in that direction.

**CS/NaDe.** Figure 6 shows the SAXS intensity for the complex phase formed by CS and NaDe. The phase has
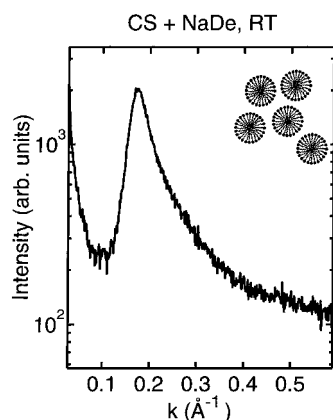
**Figure 6.** SAXS intensity of the neutral CS/De complex phase measured at room temperature. The degree of substitution of CS was 0.80. The water content of gel was 68 wt % at 60 °C.
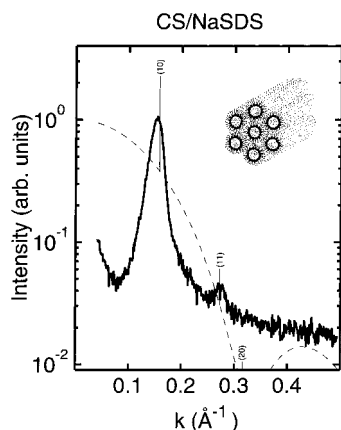


**Figure 7.** CS/DS complex at 25 °C. The vertical lines show expected reflections for $R = 12$ Å cylinders in a 2-dimensional hexagonal lattice with lattice constant 46.0 Å. The DS of starch was 0.80. The water content of gel was 52 wt % at 25 °C. The inset shows a schematic picture of the phase structure.

a clearly lower viscosity than the phases formed by surfactants with a longer chain. No long-range order is indicated by the scattering curves. At most, traces of lamellar or cylindrical structures may occur in an otherwise isotropic and random micellar solution. This indicates that, while the hydrophobic interaction between the chains is still strong enough to induce cooperative association of the surfactant with the polymer chain, a minimum surfactant chain length (12 C atoms) is required for liquid crystalline phases to occur in CS/alkanoate systems. As indicated by the relatively high surfactant concentration in the aqueous solution, (Table 4), the concentration of the complexes is low, and hence the interparticle interactions are apparently too weak to induce formation of structures with long-range order.

**CS/SDS.** As shown previously,[21] the different ionic headgroup of SDS results in interactions between CS and SDS that are different from those of the carboxylates. The position of the first two reflections (Figure 7) once again point toward a hexagonal lattice. In this case it is the (20) reflection, which is not well resolved. The lattice constant is 46 Å, and the cylinder radius is about 12 Å, which means that the starch molecules have extremely compacted conformation indicating strong CS−DS interaction.

**The Effect of the Charge Density of the CS.** Table 3 shows positions of the diffraction peaks of CS/DS for starches with lower degrees of substitution (DS). When DS = 0.72 the crystal structure is still 2-d hexagonal but the lattice constant increases. A lower DS the structure changes into a randomly ordered concentrated solution of CS/surfactant aggregates.

The same kind of phase behavior is observed for the CS/carboxylate complexes. CS/oleate when forms a well-defined 2-d hexagonal structure when DS = 0.72, but the lattice constant is larger than when DS = 0.80. When DS decreases to 0.42, the long-range order vanishes and a micellar solution is formed. For CS/Dod the structure when DS = 0.72 is the same as with DS = 0.80 (hexagonal close packing), but when the DS is decreased further (to 0.42) the ordering disappears, and a concentrated solution of CS/Dod complexes is formed.

We conclude that when the charge density of the polyelectrolyte decreases, the complex phase loses its order and behaves like a very concentrated micellar solution. The effect of decreasing charge is also to increase the lattice constant of the complexes. Indeed, as shown by Table 3, the lowering of the charge density by a relatively small amount has a surprisingly strong effect on the structure of CS/surfactant complexes. This indicates weakened interactions between the CS/surfactant aggregates.

**The Effect of Charge Equivalence.** The SAXS measurements indicate that the structure of the complex phase is quite sensitive to the charge ratio surfactant/polymer. The liquid crystalline phases of the surfactants are formed only when the total charge of the surfactant corresponds closely to the charge of the polyelectrolyte. Phase separation of the complexes takes place at lower surfactant concentrations, but the phase does not have any ordered structure until the gel is close to neutral. The same phenomenon occurs when excess surfactant is added. Then the charge of the complex is reversed and the complex begins to dissolve and loses its liquid crystalline structure.

**The Effect of Temperature.** Figure 8 shows the effect of temperature on the structure of CS/Er phase. It is lamellar until the temperature exceeds +80 °C, when another lamellar phase forms. It is well-known that the stability of lyotropic liquid crystals formed by

**Table 3. Effect of Charge Density of CS on the Structure of CS/Surfactant Complexes**

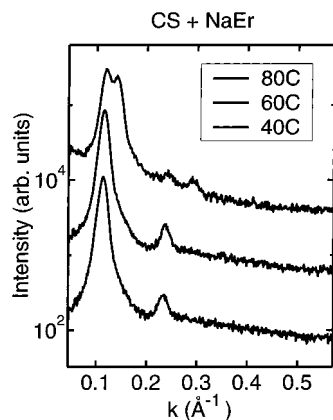| surfactant | peak positions [1/Å] | structure of complex |
|---|---|---|
| SDS | | |
| DS of CS 0.80 | 0.154, 0.274 | 2-D hexagonal |
| 0.72 | 0.130, 0.145, 0.156, 0.271 | 2-D hexagonal |
| 0.41 | 0.140 | micellar |
| NaDod | | |
| DS of CS 0.80 | 0.137, 0.145, 0.155, 0.199, 0.235, 0.255 | HCP |
| 0.72 | 0.140, 0.148, 0.0.159, 0.206 | HCP |
| NaOl | | |
| DS of CS 0.80 | 0.134, 0.228, 0.271 | 2-D hexagonal |
| 0.72 | 0.128, 0.219, 0.256 | 2-D hexagonal |
| 0.41 | 0.11 | micellar |

**Figure 8.** SAXS intensity of the neutral CS/Er complex phase measured at different temperatures from bottom to top: (40, 60, and 80 °C). The degree of substitution of CS was 0.80. The water content of gel was 54 wt % at 60 °C.

pure surfactants decreases when the temperature rises. Thus, the formation of another lamellar phase when the stability of a lamellar phase is decreased is not so surprising. Noro and Gelbart[33] have theoretically studied this kind of coexistence of two lamellar phases. They suggest that this phenomenon may be driven by two different type of forces: (1) phase separation driven by demixing of two amphiphiles within each bilayer, i.e., a purely repulsive interaction between bilayers; (2) a condensation-type phase change caused by the competition between attractive and repulsive interactions. There are several examples of both cases in the literature.[34−37] In our system it should be the increased free volume of the hydrocarbon chains that induces repulsion and by this way decreases the CS−surfactant interaction when the temperature is raised. The value of the lattice constant also decreases slightly.

Table 2 shows the positions of the diffraction peaks at different temperatures of CS/Pal complexes. The phase structure remains 2-d hexagonal in the temperature range 40−80 °C. The only detectable effect is that the lattice constant of the system decreases; i.e., the cylinders pack more closely and the water content of the phase at the two-phase boundary decreases.

The peak positions for CS/Ol are shown in Table 2. An increase in the temperature from room temperature to +80 °C has only minor effects on the structure of these complexes. The most marked effect is a slight disordering of the structure of, but it is so weak that the structure remains 2-d hexagonal. The lattice constant decreases significantly.

The structure of the CS/Dod complex phase is clearly hexagonal (hcp) from room temperature up to 60 °C (Table 2), but at higher temperatures the structure changes to $pm3n$ cubic. At 60 °C the structure is intermediate between cubic and hcp phases; it is also

possible that there are two different phases present. At 80 °C the structure is pure cubic ($pm3m$). The lattice constant decreases with increasing temperature.

Table 2 shows the SAXS peaks of CS/DS phases at different temperatures. Not much happens when the temperature is increased from room temperature to 80 °C. The structure remains 2-d hexagonal in the whole temperature range, only the lattice constant changes from 46.0 Å at room temperature to 42.9 Å at +80 °C.

In summary, these results show that when temperature raises the long-range ordering of the structures is weakened.

## Discussion

**CS/Surfactant Interactions.** The importance of different parameters affecting CS/surfactant interaction is discussed in detail in our previous articles.[19−21] The main driving forces for polymer/surfactant association are the electrostatic attraction between the polymer substituents and the surfactant headgroups as well as the hydrophobic, cooperative interaction between the hydrocarbon chains of the surfactant. Hydrophobic surfactant/polymer interactions are not important. Hydrophobic interactions between the hydrocarbon chains become very effective when the charge density of the polyelectrolyte is high, because the concentration of the oppositely charged surfactant in the vicinity of the polymer chain is high. The result is that the surfactant monomers form aggregates on the polymer at much lower concentrations than in pure solution.

In conformity with earlier studies,[38] the results presented in this paper show that the highly cooperative nature of polyelectrolyte/surfactant interactions not only leads to association between micelles and polymer but also, when the long-range electrostatic repulsion between the surfactant/polymer aggregates is reduced by charge neutralization, leads to the formation of highly ordered liquid crystalline structures. The structure of these mesophases depends on the strength of the polymer−surfactant interaction, because it depends on the concentrations at which complexes are formed.

**The Effect of Electrolyte.** Table 4 shows the composition of polymer/surfactant complexes in equilibrium with aqueous solutions at 60 °C. These results actually represent points in a four-component system, the fourth component being the low molecular weight salt, which is formed as a neutralization product when complexation occurs. In most cases, comparison of phases formed by different surfactants is made for CS with the same DS (0.8), implying that the same amount of salt is released when the CS is neutralized. Because the water content varies, the concentration of simple electrolyte varies somewhat in the different samples, but it is always quite high, so that long-range electrostatic interactions between aggregates should be es-

**Table 4. Total Concentrations of Cationic Starch and Surfactant and the Compositions of the Separate Phases in Equilibrium with Aqueous Solution at +60 °C**

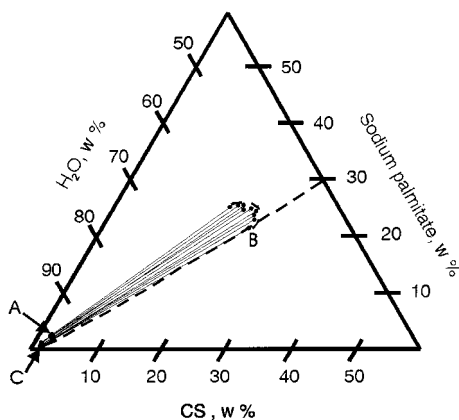| surfactant | total concn of CS (wt %) | total concn of surfactant (wt %) | CS in solution (wt %) | surfactant in solution (wt %) | CS in gel (wt %) | surfactant in gel (wt %) | water in gel (wt %) |
|---|---|---|---|---|---|---|---|
| NaDe | 1.33 | 2.01 | 0.011 | 0.0500 | 20 | 12 | 68 |
| NaDod | 1.84 | 1.40 | 0.010 | 0.0200 | 18 | 18 | 64 |
| NaPal | 1.19 | 1.06 | 0.006 | 0.0010 | 21 | 25 | 54 |
| NaOl | 1.64 | 2.04 | 0.004 | 0.0011 | 20 | 25 | 55 |
| NaEr | 1.31 | 2.66 | 0.003 | 0.0008 | 21 | 30 | 49 |
| SDS[a] | 2.00 | 1.73 | 0.005 | 0.0018 | 21 | 27 | 52 |

[a] Equilibrium at +25 °C.

**Figure 9.** Partial phase diagram of the system of CS (DS = 0.80)/NaPal/water at 60 °C. Points A indicate the compositions prepared in experiments, points B give analyzed compositions of the gel phase, and points C represent the compositions of the supernatant aqueous phase. The dashed line indicates the theoretical charge neutralization.



**Figure 10.** Partial phase diagram of the system of CS (DS = 0.80)/NaOl/water at 60 °C. Points A indicate the compositions prepared in experiments, points B give analyzed compositions of the gel phase, and points C represent the compositions of the supernatant aqueous phase. The dashed line indicates the theoretical charge neutralization.

sentially screened. Hence, the influence of other factors (polymer charge density, surfactant chain length, polar end group) can be safely deduced from the results. However, the possibility that the structures may be changed by removing the simple salt, cannot be ruled out, and it is well-known that further addition of salt may weaken surfactant/polymer interactions to the extent that no phase separation occurs.

**Comparison with Pure Surfactant Mesophases.** Pure NaPal forms a crystalline hydrate in equilibrium with dilute aqueous solution at temperatures up to ∼ 60 °C.[39] The Krafft temperature of this surfactant is ∼ 40 °C. At temperatures above 60 °C, hexagonal phase is formed in the concentration range 30−50 wt % of surfactant. At the lower phase boundary the hexagonal phase is in equilibrium with concentrated micellar solution (∼27 wt % surfactant).

Figure 9 shows the phase diagram of CS/NaPal/water system. The hexagonal phase in equilibrium with aqueous solution consists of 18−21 wt % CS, 54−62 wt % water, and 20−26 wt % surfactant. The aqueous solution contains 0.006 wt % CS, 0.001 wt % NaPal, and 0.05 mol dm$^{-3}$ NaCl. The hexagonal phase is stable at temperatures from 40 to at least 80 °C. Thus, the complexation of NaPal with CS shifts the range of existence of the NaPal hexagonal phase toward lower temperatures than for the pure surfactant. It also separates at much lower surfactant concentrations (well below the cmc of the surfactant).

Figure 10 shows the phase diagram of CS/NaOl/water system. The surfactant concentration in the complex phase varies from 20 to 26 wt %. In this concentration range, pure NaOl forms micellar solutions. Hexagonal phase is formed in the concentration range from 30 to 40 wt % and is stable from room temperature to 100 °C.[40] The same hexagonal structure is formed by the CS/Ol complex in the temperature range 25−80 °C, again in equilibrium with very dilute solution of the surfactant.

Figure 11 shows the phase diagram of CS/NaDod/water system. The surfactant concentration varies from 15 to 20 wt % in the complex phase. In this concentration range pure sodium dodecanoate forms micelles and a cubic liquid crystalline phase at temperatures below 30 °C. At higher temperatures only micellar solutions are formed. In the concentration range 30−50 wt %,



**Figure 11.** Partial phase diagram of the system of CS (DS = 0.80)/NaDod /water at 60 °C. Points A indicate the compositions prepared in experiments, points B give analyzed compositions of the gel phase, and points C represent the compositions of the supernatant aqueous phase. The dashed line indicates the theoretical charge neutralization.

NaDod forms cubic phase below 40 °C and hexagonal phase above 40 °C.[39] The phase behavior of CS/Dod complexes is quite similar, but the mesophases are stable at significantly lower surfactant concentrations and at different temperatures.
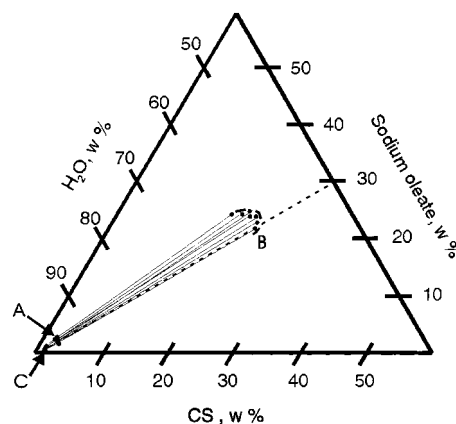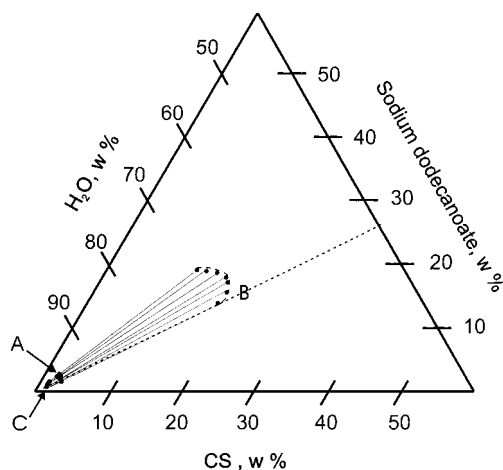
The concentration of decanoate in the phase separating from aqueous solution is quite low (<15 wt %). No long range ordering can be detected in this phase. The pure surfactant forms liquid crystalline phases only at very high surfactant concentrations.

The phase behavior of NaEr is similar to the behavior of NaPal. The Krafft points of both surfactants are well above room temperature. NaEr differs from NaPal in that the lamellar liquid crystalline phases separates from micellar solution at quite low surfactant concentrations. The structure of CS/Er complex phase is the same as for pure NaEr, but it is formed at much lower surfactant concentrations.

The hydrocarbon chain length of SDS is quite short, but the ionic sulfate group interacts strongly with the trimethylammonium groups in the CS. This strong interaction is reflected in the composition of the phase in equilibrium with aqueous solution. It contains from

25 to 30 wt % of surfactant, which is much higher than in the CS/Dod complexes, although the hydrocarbon chain lengths differ by only one carbon atom. The phase in equilibrium with aqueous solution is a 2-d hexagonal rather than a hexagonal close packing of aggregates (hcp), which implies that headgroup repulsion is more effectively screened than for CS/Dod. Pure SDS forms micellar solutions in the concentration and temperature range where the complex forms hexagonal phase.[41] In the pure SDS/water systems, above 25 °C, SDS forms hexagonal mesophase when the surfactant concentration exceeds 38 wt % and the equilibrium hexagonal phase contains 40 wt % of surfactant. In a narrow temperature range (20−25 °C) the micellar solution is in equilibrium with a crystalline hydrate of SDS.

In summary, it can be concluded that liquid crystalline phases are formed in the same sequence and with similar structures in the polyelectrolyte/surfactant system as in pure binary surfactant/water systems. The order of the phases is as a function of increasing hydrocarbon chain length of the surfactant: unordered micellar, cubic, hexagonal, cubic, and lamellar. Increasing the temperature and decreasing the charge density of the polymer has similar effect, but now the order of the phases is the opposite: lamellar, cubic, hexagonal, cubic, and micellar solution. However, the concentration of surfactant in the polyelectrolyte-containing phases is substantially lower than in pure surfactant system, and they also precipitate from solutions containing much less surfactant than in the binary system; i.e., the two-phase regions between liquid crystalline phase and solution are very wide. This shows that the effect of adding polyelectrolyte is not only an increase in the ionic strength but probably also an increase in direct binding of the polyelectrolyte to the aggregate surfaces, which reduces the electrostatic repulsion between the aggregates. This notion is further substantiated by the discussion below.

**Lattice Constants and Interparticle Distances.** Table 2 shows the lattice constants of different complex phases. These can be used as a measure of interaggregate distances. CS and erucate form a lamellar mesophase with the lattice constant 54.0 Å. The extended chain length of Er is 28 Å. This indicates that the lamellar structures have to be very close to each other because there has to be room for the CS chains between the separate lamellas.

The small-angle neutron scattering (SANS) measurements[42] at dilute solutions have shown that the surfactant molecules in complexes are incorporated into CS helix. Thus, the formation of lamellae presumably must imply some unfolding of this helix.

The extended chain length of oleate is about 23 Å. This value is very close the value of half of the Bragg distance (47 Å) of hexagonal phase of CS/Ol complex. In hexagonal geometry the Bragg distance is actually the distance between lattice planes. Thus, the lattice constant and interparticle distance is in this case 54.0 Å. It seems that the surfactant cylinders in this structure are quite close to each other, which is possible only if the CS chains are wrapped around these cylinders. This conclusion is confirmed by the SANS measurements[42] in dilute solutions.

The lattice constants in the hexagonal (hcp) CS/Dod complex phase, which is also the interparticle distance, is $a = 53$ Å and $c = 87$ Å. The length of the surfactant monomer is in this case 15.4 Å. This indicates that there

is more room between surfactant aggregates in this structure. This is also seen as a higher water content of the complex phase (Table 4).

The CS/Pal complex phase consists of hexagonally ordered cylinders. The lattice constant at room temperature, when the structure is cubic (*pm3n*), is 118 Å. At higher temperature the structure changes to 2-d hexagonal. The lattice constant and hence, the distance between the cylindrical aggregates is 55.0−52.6 Å. The extended chain length of Pal is 20.5 Å. Comparison of the interparticle distances of NaOl (54.1 Å, +40 °C) and NaPal (55.0 Å, +40 °C) shows that, despite the different chain lengths, they are quite similar. The SANS results[42] show that the radius of CS helices is about 30 Å at 70 °C. Adding of 8 mM NaPal decreases the radius to about 25 Å. Thus, it is quite obvious that CS chains take cylindrical conformation also at high concentrations with NaPal and also with NaOl. An argument in favor of this assumption is that the surfactant chain length has only a minor effect on the dimensions of cylindrical CS/surfactant aggregates. The difference in interparticle distances is also partly explained by the different water content of the two systems.

The structure of the CS/De complex phase appears to be akin to a concentrated micellar solution. The distance between the micelles is 36.0 Å at room temperature. The extended chain length of De is 13 Å so there is plenty of water between the aggregates in these complexes, as is also indicated by their analytical composition.

DS and CS form very highly viscous complexes with low water content. Depending on the temperature, the distances between the cylinders vary from 42.9 to 46.0 Å. The dimensions of a DS aggregate phase are significantly smaller, resulting in a stiffer structure, and significantly lower water content of the complex phase (Table 4).

**The Geometry of Polyelectrolyte Oppositely Charged Surfactant Aggregate Phases. Energetics of Amphiphilic Monolayers.** The structure of surfactant aggregates depends on the bending energy of surfactant layers in the aggregates. This bending energy leads to the formation of surfactant aggregates with different radii of curvature, i.e., different geometry. The bending energy, $g_c$, of the layers in an aggregate can be expressed in terms the deviations from the monolayer's preferred spontaneous curvature, $c_0$, i.e., $\Delta c_1 = c_1 - c_0$ and $\Delta c_2 = c_2 - c_0$. Thus, the bending energy is given by a two-dimensional version of Hooke's law

$$g_c = \frac{1}{2}k_c c_1^2 + \frac{1}{2}k_c c_2^2 + \bar{k}\Delta c_1 \Delta c_2 \qquad (2)$$

where $k_c$ is the bending modulus and $\bar{k}$ is a coupling constant. The bending energy depends on the intermolecular forces between the amphiphile in the monolayers, including structural forces, hydrogen bonding, electrostatic repulsion, steric repulsion, van der Waals' attractions, hydrophobic interactions, and solvation forces.

The structural force, due to the collisions between the molten hydrocarbon chains, creates an outward pressure, tending to expand the hydrocarbon moiety. This is clearly reflected in the temperature dependence of the curvature of the aggregate structures both in pure surfactant/water and CS/surfactant/water systems.

At the polar/nonpolar interface, hydrophobic interactions create an inward pressure that tends to reduce

water−oil contact. In the headgroup region there are steric, electrostatic, and hydration forces, which are expected to create a net positive outward pressure. When the outward pressure in the chain region is high the monolayer is likely to bend toward water. On basis of presently available results, the importance of hydrophobic, steric and hydration forces in the CS/surfactant/water systems are difficult to assess. However, the strong interaction between the sulfate and trimethylammonium groups in the CS/DS complexes leads to formation of aggregates with lower curvature than in corresponding CS/Dod systems, which indicates that reduction of hydrophobic interactions and solvation in the surface plays a role.

**The Electrostatic Contributions to the Bending Modulus of Mean Curvature, $k_c$.** It can be deduced from the results described above that phases similar to those formed by the pure surfactants are formed by the CS/surfactant complexes, but at considerably lower surfactant concentrations. It seems reasonable to assume that the major reason for this effect is the electrostatic interaction between the polyelectrolyte and the surfactant aggregates. Considering lamellar structures, there are three characteristic length scales: the mean membrane separation $2d$, the Debye−Hückel screening length $\kappa^{-1}$ and the Gouy−Chapman length $\lambda = e/2\pi l\sigma$, where $\sigma$ is the surface charge density, $e$ is the electronic unit charge, $l = e^2/4\pi\epsilon T$ is the Bjerrum length, and $\epsilon$ is the dielectric constant of the solvent. In the limit of high electrolyte concentration ($\kappa d > 1$ and $\kappa\lambda < 1$), the solutions of the linearized Poisson−Boltzmann equation for several geometries all indicate that the electrostatic contribution to the bending constant $k_c$ is given by[43]

$$k_c = \frac{3T}{4\pi\kappa^3 l\lambda^2} \tag{3}$$

where

$$\kappa = \left(\frac{e_o^2 \; \Sigma n_i^0 z_i^2}{\epsilon\epsilon_o kT}\right)^{1/2} \tag{4}$$

and $n_i^0$ and $z_i$ are the number concentration and valency, respectively, of ion $i$. Because $\kappa^-$ increases with increasing electrolyte concentration, the bending constant between charged particles $k_c$, decreases very rapidly when the electrolyte concentration increases. For example, when the electrolyte concentration (1:1 electrolyte) increases from 1 to 10 mM, $\kappa^{-1}$ decreases from 9.6 to 3.04 nm, and the bending constant is reduced to about 6% of its initial value.

The screening of electrostatic repulsion does, indeed, explain the reduction in the bending energy caused by ionic interactions between the polar headgroups. This is manifested in the gradual transition from micellar to saddle to lamellar phases as the concentration of surfactant in binary water/surfactant systems increases. The same effects can be obtained by adding a simple electrolyte. However, it is evident that the oppositely charged polyelectrolyte neutralizes the charges much more effectively than a simple electrolyte. Adsorption of polyelectrolyte to the monolayer (or micellar) surface neutralizes the charges by direct ion binding. This markedly reduces the electrostatic contribution to the bending energy (eq 2), and hence, the surface curvature of surfactant aggregates is changed, leading to stabili-

zation of phases with lower curvature than micelles. As eq 3 shows, the bending modulus depends strongly on the Gouy−Chapman lengths and, hence, on the charge density, i.e., the packing of the polar headgroups of the surfactant monomers. The CS has very high charge density; therefore, the association of surfactant aggregates with CS chains with high charge, via charge neutralization, results in a very effective shortening of $\lambda$ and, hence, also a lower bending energy and a closer packing of surfactant monomers in aggregates of low curvature. Similar conclusions of effect of electrolyte concentration on structure of polyelectrolyte−surfactant complexes were reached in a recent study of sodium poly(acrylate)/cetyltrimethylammonium bromide systems.[44]

When the ionic strength increases, the phase boundaries of the lyotropic liquid crystalline phases move toward lower surfactant concentrations. They also shift to higher temperatures, indicating increased stability of the surfactant aggregates. However, this effect is much weaker than the effect of adding a polyelectrolyte. For instance, the phase diagram of the NaPal/NaCl/water system[45] shows that addition of up to 5 wt % of NaCl to a 1 wt % NaPal solution does not cause any phase changes. In our investigation, the initial NaPal concentration of the CS/NaPal sample was 1.06 wt % and the CS concentration 1.19 wt % (Table 4). The estimated effect of CS on the ionic strength corresponds approximately to 0.1 wt % of added NaCl. This indicates very clearly that the addition of a polyelectrolyte has a much stronger effect than the addition of a simple electrolyte.

Because the formation of more or less neutral complexes occurs when the polycation associates with an anionic surfactant, there is also an ionic strength effect due to the release of simple ions from the polyelectrolyte and the micelles. This could explain part of the detected shift of the phase boundaries and areas of liquid crystalline phases of CS/surfactant complexes, but it is clear from the discussion above that this effect is minor.

**References and Notes**

(1) *Interactions of Surfactants with Polymers and Proteins*; Goddard, E. D., Ananthapadmanadhan, K. P., Eds.; CRC Press: Boca Raton, FL, 1993.
(2) Hayakawa, K.; Kwak, J. C. T. In *Cationic Surfactants*, 2nd ed.; Rubingh, N. D., Holland, P. M., Eds.; Marcel Dekker: New York, 1991; pp 189−248.
(3) Saito, S. In *Nonionic Surfactants*; Schick, M. J., Ed.; Marcel Dekker: New York, 1991; pp 881−926.
(4) Robb, I. D. In *Anionic Surfactants−Physical Chemistry of Surfactant Action*; Lucassen-Reynders, E., Ed.; Marcel Dekker: New York, 1981; pp 109−142.
(5) Harada, A.; Nozakura, S. *Polym Bull.* **1984**, *11*, 175−178.
(6) Chen, L.; Yu, S.; Kagami, Y.; Gong, J.; Osada, Y. *Macromolecules* **1998**, *31*, 787−794.
(7) Kim, R.; Ishizawa, M.; Gong, J.; Osada, Y. *J. Polym. Sci. A* **1999**, *37*, 635−644
(8) Korobko, T. A.; Izumrudov, V. A.; Zezin, A. B.; Kabanov, V. A. *Polym. Sci.* **1994**, *36*, 179−183.
(9) Khandurina, Y. V.; Rogacheva, V. B.; Zezin, A. B.; Kabanov, V. A. *Polym. Sci.* **1994**, *36*, 184−188.

(10) Khandurina, Y. V.; Dembo, A. T.; Rogacheva, V. B.; Zezin, A. B.; Kabanov, V. A. *Polym. Sci.* **1994**, *36,* 189−194.

(11) Khandurina, Y. V.; Rogacheva, V. B.; Zezin, A. B.; Kabanov, V. A. *Polym. Sci.* **1994**, *36*, 195−199.

(12) Bakeev, K. N.; Yang, M. S.; MacKnight, W. J.; Zezin, A. B.; Kabanov, V. A. *Macromolecules* **1994**, *27*, 300.

(13) Hansson, P. *Langmuir* **1998**, *14*, 4059−4064.

(14) Ilekti, P.; Piculell, L.; Tounilhac, F.; Cabane, B. *J. Phys. Chem. B* **1998**, *102*, 344−351.

(15) Kosmella. S.; Kötz, J.; Friberg, S. E.; MacKay, R. *Colloids Surf. A* **1996**, *112***,** 227−231.

(16) Ruppelt, D.; Kötz, J.; Jaeger, W.; Friberg, S. E.; MacKay, R. *Langmuir* **1997**, *13*, 3316−3319.

(17) Zhou, S.; Burger, C.; Yeh, F.; Chu, B *Macromolecules* **1998**, *31*, 8157−8163.

(18) Zhou, S.; Yeh, F.; Burger, C.; Chu, B. *J. Phys. Chem. B* **1999**, *103*, 2107−2112.

(19) Merta, J.; Stenius, P. *Colloid Polym. Sci.* **1995**, *273*, 974−983.

(20) Merta, J.; Stenius, P. *Colloids Surf. A*: *Physicochem. Eng. Asp.* **1997**, *122*, 243−255.

(21) Merta, J.; Pirttinen, E.; Stenius, P. *J. Dispersion Sci. Technol.* **1999**, *20*, 677−697.

(22) Goddard, E. D.; Hannan, R. B. *J. Colloid Interface Sci.* **1976**, *55*, 73−79.

(23) Goddard, E. D.; Hannan, R. B. *J. Am. Oil Chem. Soc.* **1977**, *54*, 561−566.

(24) Rutenberg, M. W.; Solarek, D. Starch derivates: Production and uses, In *Starch Chemistry and Technology*; Whistler, R. L., Miller, J. N., Paschall, E. F., Eds.; Academic Press Inc.: Orlando, FL, 1984; pp 311−388.

(25) Bradstreet, R. B. *The Kjeldahl Method for Organic Nitrogen*; Academic Press: New York, 1965.

(26) *International Tables for Crystallography*; Hahn, T.; Ed.; D. Reidel Publishing Co.: Dordrecht, The Netherlands, 1985; 128 pp.

(27) Eriksson, P.-O.; Lindblom, G.; Arvidson, G. *J. Phys. Chem.* **1987**, *91*, 846−853.

(28) Mariani, P.; Luzzati, V.; Delacroix, H. *J. Mol. Biol.* **1988**, *204*, 165−189.

(29) Fontell, K.; Fox, K. K.; Hansson, E. *Mol. Cryst. Liq. Cryst., Lett. Sect.* **1985**, *1* (1−2), 9−17.

(30) Chirova, G. A.; Markina, Z. N. *Mezhdunar. Kongr. Poverkhn.-Akt. Veshchestvam, 7th* **1978**, *2* (II), 975−986.

(31) Rancon, Y.; Charvolin, J. *J. Phys. Chem.* **1988**, *92*, 2646−2651.

(32) Hoinkis, E. *Chem. Phys. Carbon* **1997**, *25*, 71−241.

(33) Noro, M. G.; Gelbart, W. M. *J. Chem. Phys.* **1999**, *111*, 3733−3743.

(34) Lis, L. J.; Parsegian, V. A.; Rand, R. P. *Biochemistry* **1981**, *20*, 1761−1770.

(35) Dubois, M.; Zemb, T.; Belloni, L.; Delville, A.; Levitz, P.; Setton, R. *J. Phys. Chem.* **1992**, *96*, 2278−2286.

(36) Khan, A.; Jonsson, B.; Wennerstrom, H. *J. Phys. Chem.* **1985**, *89*, 5180−5184.

(37) Fontell, K.; Ceglie, A.; Lindman, B.; Ninham, B. *Acta Chem. Scand.* **1986**, *A40*, 247−256.

(38) See, for example, Jönsson, B.; Lindman, B.; Holmberg, K.; Kronberg, B. *Surfactants and Polymers in Aqueous Solution*; Wiley: New York, 1998, Chapter 3.

(39) Madelmont, C.; Perron, R. *Colloid Polym. Sci.* **1976**, *254*, 581−595.

(40) Vold, R. D. *J. Phys. Chem.* **1939**, *43*, 1213−1231.

(41) Kekicheff, P.; Grabielle-Madelmont, C.; Ollivon, M. *J. Colloid Interface Sci.* **1989**, *131*, 112−132.

(42) Merta, J.; Garamus, V.; Willumeit, R.; Kuklin, A.; Stenius, P. *Langmuir* **2000**, *16*, 10061−10068.

(43) Harden, J. L.; Marques, C.; Joanny, J.-F. *Langmuir* **1992**, *8*, 1170−1175.

(44) Ilekti, P.; Martin, T.; Cabane, B.; Piculell, L. *J. Phys. Chem.* **1999**, *103*, 9831−9840.

(45) Laughlin, R. G. *The Aqueous Phase Behaviour of Surfactants*; Academic Press: New York, 1994.